**Proceedings of the 17th World Congress**
**The International Federation of Automatic Control**
**Seoul, Korea, July 6-11, 2008**

# On the stability and biasedness of the cross-relation blind thermocouple characterisation method

**Seán F. McLoone*, Peter C. Hung*, George W. Irwin**, Robert J. Kee****

*Department of Electronic Engineering, National University of Ireland Maynooth, Maynooth, Co. Kildare, Ireland (Tel:+353-1-708-6313; e-mail: {sean.mcloone, phung}@eeng.nuim.ie)
**Virtual Engineering Centre, Queen's University Belfast, Belfast, BT9 5HN, Northern Ireland (e-mail: g.irwin@ee.qub.ac.uk, r.kee@qub.ac.uk)

**Abstract:** The *in situ* characterisation of thermocouple sensors is a challenging problem. Recently the authors introduced a novel blind characterisation technique based on the cross-relation method of blind identification that allows *in situ* characterisation of temperature measurement probes consisting of two-thermocouple sensors with differing time constants. While the technique has a number of advantages over competing methods, including low estimation variance and no need for *a priori* estimation of the time constant ratio, it was found to be positively biased and becomes unstable at high noise levels. In this paper the origin of the stability issues and bias are analysed. It is shown that an alternative normalised cost function formulation, which eliminates the stability problem, results in negatively biased time constant estimates at high noise levels. Further, it is demonstrated that this bias is less significant when temperature variations are broadband. All results are verified using Monte-Carlo simulations.

## 1. INTRODUCTION

In general, the frequency response of thermocouples used to measure the temperature in a liquid or gas flow can be adequately described by a first-order lag model with time constant, $\tau$ , and unity gain (Tsuji *et al.*, 1992). This simplified model can be written mathematically as

$$T_{\mathrm{f}}(t) = T(t) + \tau \frac{dT(t)}{dt}, \qquad (1)$$

where $T_{\mathrm{f}}$ is the true temperature of the flow and $T$ is the thermocouple output measurement. The time constant, $\tau$ , is a function of the thermocouple wire diameter $d$ and the flow velocity $v$, that is

$$\tau \propto \sqrt{d^3 / v} \,. \qquad (2)$$

While $\tau$ can often be determined *a priori*, this is not feasible in varying gas/liquid flow environments (e.g. in the exhaust of an internal combustion engine) due to its dependency on $v$. Consequently, *in situ* characterisation is needed.

*In situ* characterisation is a very challenging problem since only the thermocouple output measurements are available, i.e. we do not have access to the input signal. In the field of system identification this is referred to as a blind identification problem. In the absence of additional information the problem is in fact unsolvable. Various methods have been proposed over the years which exploit additional information to obtain blind identification characterisation algorithms. Much of this work has been done in the signal processing community in the context of channel equalization and image restoration problems. Broadly speaking these methods can be classified as either deterministic or non-deterministic techniques. The former rely on structural redundancy when using multiple sensors, while the latter exploit knowledge of the statistics of the input to the sensor.

In addressing the problem of *in situ* thermocouple characterisation, several researchers have independently developed techniques which essentially fall into the former category. Pfriem (1936) was the first to observe that using two thermocouples with differing time constants to measure the same temperature provided sufficient information to allow *in situ* characterisation of both thermocouples. His method relied on *a priori* knowledge of the ratio of the time constants, $\alpha$ , defined as

$$\alpha = \frac{\tau_1}{\tau_2}, \qquad \alpha < 1, \qquad (3)$$

a parameter which is approximately invariant to flow velocity fluctuations (Kee *et al.* 1999). (In (3) the subscripts 1 and 2 refer to the two thermocouples with different $\tau$ values). Independently, Strahle and Muthukrishman (1976) and Cambray (1986) developed similar ideas. More recently several researchers have developed more sophisticated identification algorithms which can characterise the two-thermocouple probe without requiring knowledge of the time constant ratio. These include Tagawa *et al.* (1998, 2003) who developed a number of frequency domain techniques and Hung *et al.* (2005) who developed difference equation time domain algorithms. All these developments appear to have been made in isolation of the work done by the signal processing community on blind system identification.

In contrast, Hung *et al.* (2007) proposed a two-thermocouple probe (TTP) characterisation technique based on a

deterministic blind identification method from the signal processing community, referred to as the cross-relation (CR) method (Liu *et al.*, 1993). The algorithm was shown to have several advantages over competing methods including low estimation variance and no need for *a priori* estimation of the time constant ratio. However, Monte-Carlo analysis showed that the algorithm was positively biased in the presence of measurement noise and became unstable at high noise levels.

In this paper the origin of the stability issues and bias are explored in detail. It is shown that an alternative normalised cost function formulation, which eliminates the stability problem, results in negatively biased time constant estimates at high noise levels. Further, it is demonstrated that this bias is less significant when temperature variations are broadband. All results are verified using Monte-Carlo simulations.

Following some preliminaries in Section 2 a brief overview of the CR characterisation technique is provided in Section 3. The stability problem and its solution are demonstrated in Section 4. A mathematical analysis of the bias introduced in the MSE and NSME formulations by measurement noise is presented in Section 5. Monte-Carlo simulation results in support of this analysis are then presented in Section 6. Discussion and conclusions follow in the final section.

## 2. PRELIMINARIES

Throughout the paper analysis will be performed with the aid of two simulated data sets generated in MATLAB® using the block diagram shown in Fig. 1. Here two thermocouples, modelled as low-pass filters with unity gain and time constants, $\tau_1 = 23.8$ ms and $\tau_2 = 116.8$ ms, respectively, are connected to a common input representing the fluctuating gas or liquid temperature signal. The first simulated signal represents sinusoidal temperature variations and is defined as

$$T_{\mathrm{f}}(t) = 16.5\sin(20\pi t) + 50.5\,, \qquad (4)$$

while the second is a broadband signal generated using Matlab's normally distributed random signal generator. Samples of each signal, along with the corresponding thermocouple measurements are given in Fig. 2. Each data set consists of 1500 samples at a sample rate of 2 ms collected after initial condition transients have decayed away.

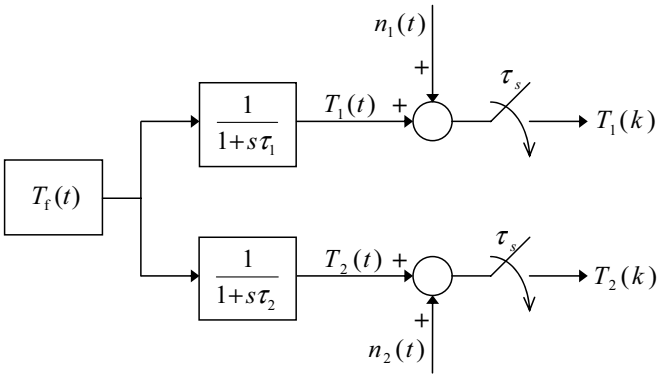


Fig. 1. Block diagram representation of the simulated two-thermocouple measurement system

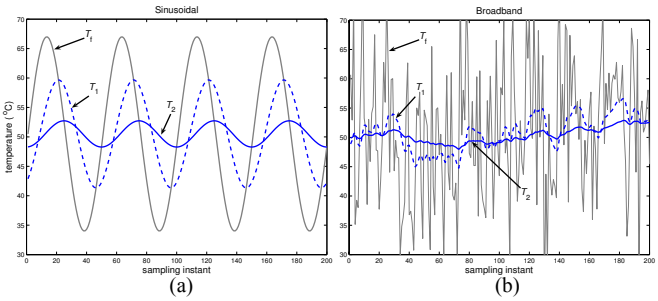


Fig. 2. Simulated case studies: (a) sinusoidal; and (b) broadband temperature fluctuations

When adding zero-mean white Gaussian measurement noise to each thermocouple output, the amount of noise introduced is quantified in terms of the noise level, $L_e$, defined as

$$L_e = \sqrt{\frac{\mathrm{var}(n_i)}{\mathrm{var}(T_{\mathrm{f}})}}\cdot 100\% \quad , \quad i = 1, 2\,. \qquad (5)$$

In all experiments noise of equal power is added to each thermocouple, i.e. $\mathrm{var}(n_1) = \mathrm{var}(n_2)$.

## 3. BLIND CHARACTERISATION

To exploit the information provided by output measurements from two systems of known structure but unknown parameters, the method of cross-relation (CR) proposed by Liu *et al.* (1993) can be employed. The implementation of the method for a two-thermocouple probe is illustrated in Fig. 3. Here, the two thermocouple output signals $T_1(t)$ and $T_2(t)$ are passed through two different synthetic thermocouples modelled by first-order transfer functions:

$$\hat{G}_1(s) = \frac{1}{1+s\hat{\tau}_1} \quad \text{and} \quad \hat{G}_2(s) = \frac{1}{1+s\hat{\tau}_2}\,, \qquad (6)$$

where $\hat{G}_1(s)$ and $\hat{G}_2(s)$ are estimates of the transfer functions of the two thermocouples $G_1(s)$ and $G_2(s)$. A mean-square-error cost function

$$J_{\mathrm{MSE}}(\hat{\tau}_1, \hat{\tau}_2) = E[e^2]\,, \qquad \forall\ \hat{\tau}_1, \hat{\tau}_2\,, \qquad (7)$$

where

$$e = T_{12}(t) - T_{21}(t)\,, \qquad (8)$$

is then minimised to give estimates of $\hat{\tau}_1$ and $\hat{\tau}_2$.

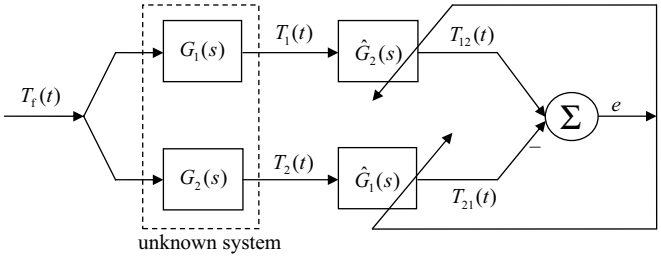


Fig. 3. Two-thermocouple cross-relation characterisation

Commutation is a fundamental requirement for the CR property underpinning the method, hence, the thermocouple models are both assumed to be linear. In addition, the thermocouples are assumed to be experiencing the same environmental conditions, i.e. measuring the same flow element with uniform temperature and velocity. Two further conditions are necessary in order for the time constants to be identifiable: (i) the input temperature signal, $T_f(t)$, must be persistently exciting; (ii) the diameters of the two thermocouples must be different (Xu *et al.*, 1995), that is:

$$d_1 \neq d_2 \quad \Rightarrow \quad \tau_1 \neq \tau_2 . \tag{9}$$

Finally, while recursive implementations of the CR method are possible, here only the constant parameter implementation is considered, hence $v$ is assumed to be constant over the characterisation interval, such that $\tau_1$ and $\tau_2$ are time-invariant.

While it is clear that the cross-relation cost function $J_{\text{MSE}}(\hat{\tau}_1, \hat{\tau}_2)$ is ideally zero when $\hat{\tau}_1 = \tau_1$ and $\hat{\tau}_2 = \tau_2$, in practice it will not be possible to match $T_{12}$ exactly with $T_{21}$. This is due to factors such as measurement noise on thermocouple outputs and violations of the assumption that the two thermocouples are experiencing identical environmental conditions. A 3-D surface plot and contour map of the $J_{\text{MSE}}$ cost function for the sinusoidal case study are shown in Fig. 4(a). Due to its non-quadratic nature, $J_{\text{MSE}}$ cannot be minimised using linear techniques such as least squares. More importantly, it is multimodal with a second minimum at $\hat{\tau}_1 = \hat{\tau}_2 = \infty$. This is because the low-pass filters in (6) behave as open-circuits when the time constants are infinite, hence, $e$ will always be zero. It should be noted that the minimum at infinity exists irrespective of the noise conditions or any violations of the modelling assumptions and is in fact the global minimum.

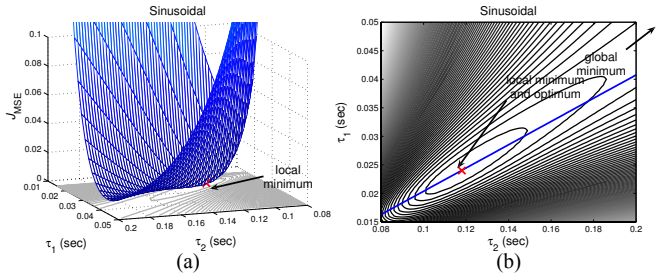


(a) (b)

Fig. 4. (a) $J_{\text{MSE}}$ for the sinusoidal case study using noiseless thermocouple measurements; (b) projection of the 1-D CR cost function onto the 2-D cost function contour map

Without loss of generality, to enhance the clarity of graphical representations and simplify the mathematical expressions presented in the following sections, analysis will be restricted to a one-dimensional implementation of the CR method. This is obtained by exploiting *a priori* knowledge of the time constant ratio $\alpha$ (3) to eliminate one of the time constants, that is

$$J_{\text{MSE}}(\hat{\tau}_1, \hat{\tau}_2) \rightarrow J_{\text{MSE}}(\alpha\hat{\tau}_2, \hat{\tau}_2) \rightarrow J_{\text{MSE}}(\hat{\tau}_2) . \tag{10}$$

The resulting 1-D CR cost function corresponds to a vertical section through the 2-D cost function along the line radiating from the origin through the true time constants. This is illustrated graphically in Fig. 4(b).

## 4. CROSS-RELATION COST FUNCTION INSTABILTY

In Hung *et al.* (2007) the authors discovered that the minimum at infinity significantly impacts on the stability of the CR scheme. In addition to the obvious problem of bounding the desired local minimum when using gradient based optimisation algorithms, it turns out that the local minimum disappears as the noise level increases with the result that the time constant estimates diverge to infinity.

Figure 5 shows a plot of the 1-D MSE CR cost function for various noise levels and clearly demonstrates how the CR method breaks down as the noise level increases. As the noise increases the local minimum becomes more and more shallow and eventually disappears for $L_e \approx 7$.

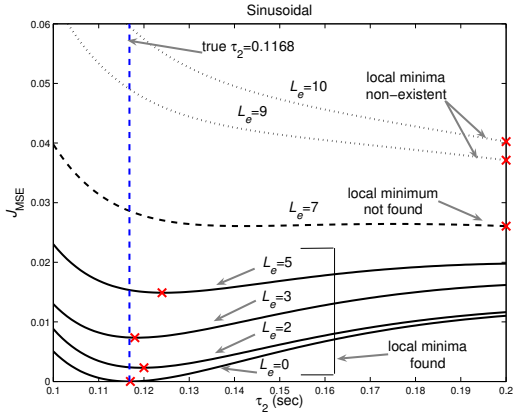


Fig. 5. Plot of the 1-D MSE CR cost function for different noise levels, $L_e$

To counter these problems Hung *et al.* (2007) proposed an alternative normalised MSE cost function formulation which eliminates the minimum at infinity by penalising large time constants, that is:

$$J_{\text{NMSE}}(\hat{\tau}_1, \hat{\tau}_2) = \frac{E[e^2]}{0.5[\text{var}(T_{12}) + \text{var}(T_{21})]} . \tag{11}$$

The 3-D surface plot and contour map for this cost function are given in Fig. 6(a). The corresponding 1-D cost function is plotted in Fig. 6(b) and clearly shows that the NMSE eliminates the stability problem. This is verified in Fig. 7 which shows the 1-D NMSE CR cost function for different noise levels, $L_e$.

In addition to the stability problems Hung *et al.* (2007) observed that $J_{\text{MSE}}$ produced positively biased parameter estimates in the presence of noise while those produced by $J_{\text{NMSE}}$ were negatively biased. Note, that these patterns are also evident in Figs. 5 and 7. In the next section the origin of these biases will be investigated with the aid of a mathematical analysis of noise corrupted CR cost functions.

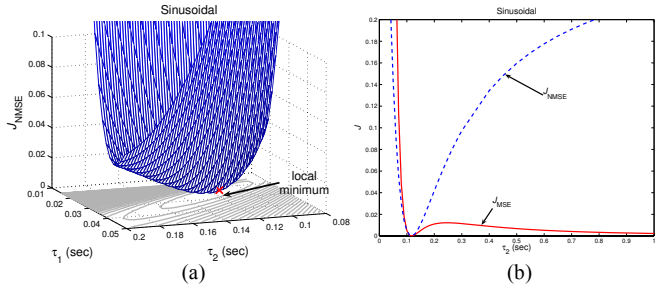


Fig. 6. Plot of (a) $J_{\mathrm{NMSE}}$ for the sinusoidal case study using noiseless thermocouple measurements; (b) the 1-D MSE and NMSE CR cost functions

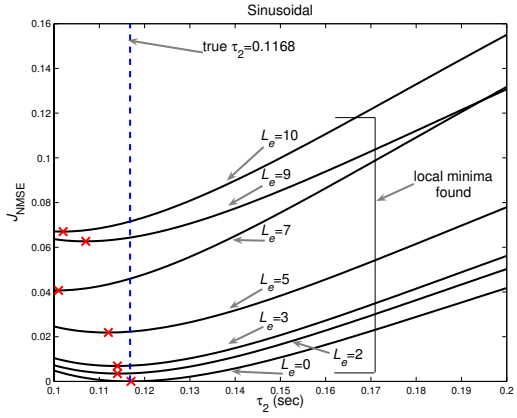


Fig. 7. Plot of the 1-D NMSE CR cost function for different noise levels, $L_e$

## 5. ANALYSIS OF BIAS

### *5.1 Noise Corrupted MSE Cost Function*

A mathematical expression for the effect of noise on the MSE CR cost function can be developed as follows. When dealing with linear systems superposition applies, therefore the cross-relation signals $T_{12}$ and $T_{21}$ in Fig. 3 can be expanded as

$$T_{12} = T_{1\mathrm{f}} + n_{1\mathrm{f}}\,,\ T_{21} = T_{2\mathrm{f}} + n_{2\mathrm{f}} \tag{12}$$

where $T_{1\mathrm{f}}$ and $T_{2\mathrm{f}}$ are the filtered noise free thermocouple signals and $n_{1\mathrm{f}}$ and $n_{2\mathrm{f}}$ are the corresponding filtered noise terms. The noise corrupted version of $J_{\mathrm{MSE}}$, denoted $\widetilde{J}_{\mathrm{MSE}}$, can then be expressed as

$$\begin{aligned}\widetilde{J}_{\mathrm{MSE}} &= E[(T_{1\mathrm{f}} - T_{2\mathrm{f}})^2] + E[n_{1\mathrm{f}}^2] + E[n_{2\mathrm{f}}^2] \\ &= J_{\mathrm{MSE}} + E[n_{1\mathrm{f}}^2] + E[n_{2\mathrm{f}}^2].\end{aligned} \tag{13}$$

The first term is the mean-square-error (MSE) due to incorrect time constant estimates and is independent of the noise present in the data. The second and third terms are the contributions to the cost function error by the filtered measurement noise.

The expression $E[n_{1\mathrm{f}}^2]$ is the noise power of the filtered noise signal, $n_{1\mathrm{f}}$. For zero-mean white noise this can be expressed as the product of the input noise power density $\eta_0^2$ and the noise bandwidth of the low pass filter, $\hat{G}_2(s)$. Since noise bandwidth is proportional to the 3 dB bandwidth it follows that

$$E[n_{1\mathrm{f}}^2] = k_1/\hat{\tau}_2\,. \tag{14}$$

Similarly, $E[n_{2\mathrm{f}}^2]$ can be expressed as

$$E[n_{2\mathrm{f}}^2] = k'/\hat{\tau}_1 = k'/(\alpha\hat{\tau}_2) = k_2/\hat{\tau}_2\,. \tag{15}$$

Here, $k_1$, $k'$ and $k_2$ are scalars arising from input signal noise power, noise bandwidth, non-ideal filter correction and time constant ratio factors. Substituting these expressions into (13) gives

$$\widetilde{J}_{\mathrm{MSE}} = J_{\mathrm{MSE}} + k_n/\hat{\tau}_2\,, \tag{16}$$

where $k_n = k_1 + k_2$. Thus, the noise term on the MSE cost function,

$$N_{\mathrm{MSE}} = k_n/\hat{\tau}_2\,, \tag{17}$$

is inversely proportional to the time constant estimate. Scalar, $k_n$, is proportional to the noise power and therefore increases as a function of the square of the noise level.

### *5.2 Noise Corrupted NMSE Cost Function*

Noting that for zero mean signals, $\mathrm{var}(T_{if}) \equiv E[T_{\mathrm{if}}^2]$, the noise corrupted version of the NMSE cost function can be expressed as

$$\widetilde{J}_{\mathrm{NMSE}} = \frac{J_{\mathrm{MSE}} + k_n/\hat{\tau}_2}{0.5[\mathrm{var}(T_{1\mathrm{f}}) + \mathrm{var}(T_{2\mathrm{f}}) + k_n/\hat{\tau}_2]}\,. \tag{18}$$

For a sinusoidal input signal with frequency $\omega$ radians/sec, the filter output signal power can be expressed as

$$\mathrm{var}(T_{1\mathrm{f}}) = \frac{\mathrm{var}(T_1)}{1 + (\omega\hat{\tau}_2)^2}\,. \tag{19}$$

Therefore, provided $\omega\hat{\tau}_2 >> 1$ the decay in the cross-relation signal power with $\hat{\tau}_2$ can be approximated as

$$\mathrm{var}(T_{1\mathrm{f}}) = c_1/\hat{\tau}_2{}^2\,. \tag{20}$$

Similarly, $\mathrm{var}(T_{2\mathrm{f}})$ can be expressed as

$$\mathrm{var}(T_{2\mathrm{f}}) = c_2/\hat{\tau}_2{}^2\,. \tag{21}$$

Here, $c_1$ and $c_2$ are constants. Substituting (20) and (21) into (18) gives

$$\widetilde{J}_{\mathrm{NMSE}} = \frac{J_{\mathrm{MSE}} + k_n/\hat{\tau}_2}{0.5[c_p/\hat{\tau}_2{}^2 + k_n/\hat{\tau}_2]}\,, \tag{22}$$

where $c_p = c_1 + c_2$. Expressing the cost function in the form

$$\widetilde{J}_{\mathrm{NMSE}} = J_{\mathrm{NMSE}} + N_{\mathrm{NMSE}} \tag{23}$$

yields the NMSE noise term as

$$N_{\mathrm{NMSE}} = 2\frac{k_n}{c_p}\hat{\tau}_2\left(\frac{c_p - J_{\mathrm{MSE}}\hat{\tau}_2^{\,2}}{c_p + k_n\hat{\tau}_2}\right). \quad (24)$$

Noting that near the true time constant estimates $J_{\mathrm{MSE}} \approx 0$, and provided $c_p >> k_n\hat{\tau}_2$, this can be approximated as

$$N_{\mathrm{NMSE}} \approx 2\frac{k_n}{c_p}\hat{\tau}_2 = k_p\hat{\tau}_2 \quad (25)$$

and hence,

$$\tilde{J}_{\mathrm{NMSE}} \approx J_{\mathrm{NMSE}} + k_p\hat{\tau}_2 . \quad (26)$$

For signals containing multiple frequencies the expression in (19) is no longer valid. Instead the output power is obtained by integrating (19) over the frequency spectrum of the input signal. In the most general case of a white noise (broadband) signal

$$\mathrm{var}(T_{\mathrm{lf}}) \to c_1/\hat{\tau}_2 \quad (27)$$

and the noise term on the NMSE cost function reduces to

$$N_{\mathrm{NMSE}} = 2\frac{k_n}{c_p}\left(\frac{c_p - J_{\mathrm{MSE}}\hat{\tau}_2}{c_p + k_n}\right), \quad (28)$$

which is approximately constant in the vicinity of the true time constant estimates, i.e.

$$N_{\mathrm{NMSE}} \approx 2\frac{k_n}{c_p} = k_p , \quad (29)$$

and hence,

$$\tilde{J}_{\mathrm{NMSE}} \approx J_{\mathrm{NMSE}} + k_p . \quad (30)$$

### *5.3 Bias on Time Constant Estimates*

From these expressions the bias on the time constant estimates can be predicted. Differentiating each cost function with respect to $\hat{\tau}_2$ gives

$$\frac{\partial\tilde{J}}{\partial\hat{\tau}_2} = \frac{\partial J}{\partial\hat{\tau}_2} + \frac{\partial N}{\partial\hat{\tau}_2} . \quad (31)$$

At the true minimum $\partial J/\partial\hat{\tau}_2 = 0$, but because of the noise term *N*, the noise corrupted cost function gradient may not be zero. If $\partial N/\partial\hat{\tau}_2 > 0$ $\tilde{J}$ will have a lower value, and hence a minimum, to the left of the true minimum point, i.e. it will generate negatively biased estimates. Alternatively, by a similar argument if $\partial N/\partial\hat{\tau}_2 < 0$ time constant estimates will be positively biased. Unbiased estimates will only be obtained if $\partial N/\partial\hat{\tau}_2 = 0$. Clearly, therefore, $\tilde{J}_{\mathrm{MSE}}$ will be positively biased for all signals and $\tilde{J}_{\mathrm{NMSE}}$ will be negatively biased for narrow band signals, but with a tendency to become unbiased for broadband signals.

## 6. MONTE-CARLO SIMULATIONS

To verify the statistical properties of the MSE and NMSE CR algorithms, a set of Monte-Carlo simulations were performed for the sinusoidal and broadband case studies over a range of noise levels. For each noise level algorithm performance was assessed in terms of the percentage error in estimating $\tau_2$, that is

$$e_\tau = \frac{\hat{\tau}_2 - \tau_2}{\tau_2}\cdot 100\% . \quad (32)$$

The mean and standard deviation of this estimation error, computed over 100 simulation runs, are recorded in Table 1 and Table 2 for the sinusoidal and broadband signals, respectively. The percentage of runs for which the MSE CR algorithm converged at each noise level is also recorded. In the cases where not all runs converged the statistics were computed based only on the converged subset. In the sinusoidal case study the MSE CR algorithm failed to converge for noise levels of 8% and above, while in the broadband case study complete breakdown did not occur until the noise level exceeded 25%.

**Table 1. Mean and (standard deviation) of time constant estimation errors – sinusoidal case study**

| Noise Level | 1 | 5 | 6 | 7 | 10 | 15 | 20 |
|---|---|---|---|---|---|---|---|
| % of runs converged | 100 | 100 | 99 | 40 | 0 | 0 | 0 |
| MSE | 0.17 (0.50) | 6.72 (2.90) | 11.42 (4.67) | 14.45 (4.63) | * | * | * |
| NMSE | -0.28 (0.45) | -5.44 (2.42) | -6.76 (3.12) | -9.08 (3.64) | -14.98 (4.52) | -26.98 (6.01) | -37.84 (6.30) |

* algorithm divergence for all simulation runs.

**Table 2. Mean and (standard deviation) of time constant estimation errors – broadband case study**

| Noise Level | 1 | 5 | 6 | 7 | 10 | 15 | 20 |
|---|---|---|---|---|---|---|---|
| % of runs converged | 100 | 100 | 100 | 100 | 100 | 96 | 45 |
| MSE | 0.27 (0.65) | 3.61 (3.59) | 4.43 (3.74) | 6.15 (5.20) | 13.54 (6.67) | 29.14 (10.33) | 54.53 (13.01) |
| NMSE | -0.03 (0.70) | 0.38 (3.26) | 0.35 (4.04) | 0.00 (4.40) | 0.59 (6.68) | 0.97 (9.57) | -0.43 (12.98) |

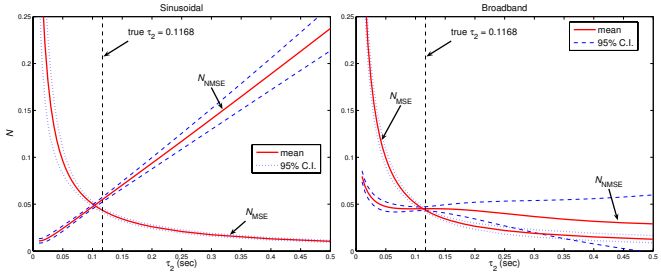


Fig. 8. MSE and NMSE noise terms (*N*) for: (a) sinusoidal; and (b) broadband temperature fluctuations

To further validate the results of the mathematical analysis the noise terms (as a function of $\tau_2$) were estimated at a

noise level of 8%, by subtracting the noise free cost functions from the noise corrupted versions ( $N = \widetilde{J} - J$ ) and averaging over 36 Monte-Carlo simulation runs. These estimates are plotted in Fig. 8 (a) and (b) for the sinusoidal and broadband signals, respectively.

## 7. DISCUSSION AND CONCLUSIONS

Overall the results are in excellent agreement with the deductions of the mathematical analysis. The estimate of MSE noise term ($N_{\mathrm{MSE}}$), which is identical for both signal types, is inversely proportional to $\hat{\tau}_2$ with a constant of proportionality, $k_n \approx 0.005$ . For the sinusoidal data sets the NMSE noise term ($N_{\mathrm{NMSE}}$) is approximately linear with a slope $k_p \approx 0.45$ , where as in the case of the broadband signal $N_{\mathrm{NMSE}}$ is almost constant in the vicinity of $\tau_2$ . In addition, the Monte-Carlo simulation results in Tables 1 and 2 confirm the predicted bias effects arising from the different noise profiles, namely a positive bias with $\widetilde{J}_{\mathrm{MSE}}$ for both signal types, a negative bias with $\widetilde{J}_{\mathrm{NMSE}}$ for the sinusoidal signal and the absence of a bias in the case of the broadband signal.

The Monte-Carlo results also highlight the instability of the MSE CR algorithm. The nature of this instability (and also the bias on estimates) can easily be understood by plotting *J*, *N* and *J*+*N* on the same axis for each of the algorithm-problem combinations as illustrated in Fig. 9.

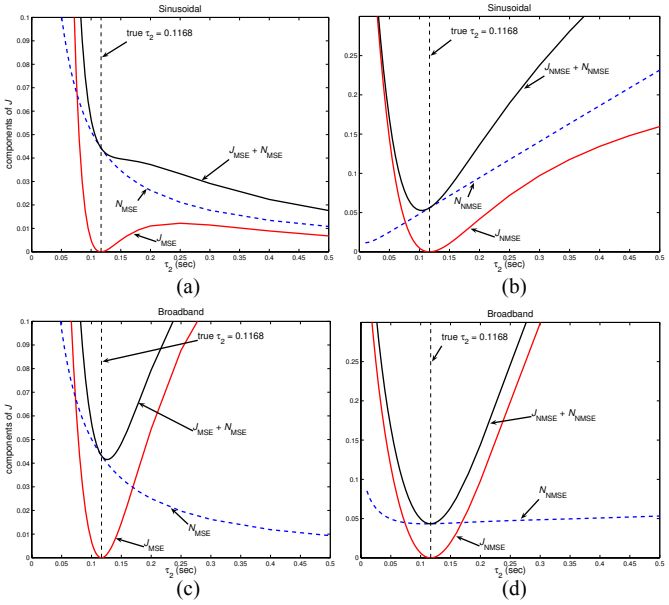


Fig. 9. Plots of *J*, *N* and *J*+*N*, at a noise level of 8% for: (a) MSE (sinusoidal data); (b) NMSE (sinusoidal data); (c) MSE (broadband data); and (d) NMSE (broadband data)

From Fig 9(a) and 9(c) it can be seen that the effect of the $1/\hat{\tau}_2$ noise term is to introduce a positive bias in the estimate of $\tau_2$ . When this bias exceeds the basin of attraction of the noise free minimum the local minimum disappears leaving only the global minimum at infinity. In contrast the NMSE cost function is convex and therefore stable at all noise levels. However, in this instance the noise term has a positive slope for narrowband signals. This has the effect of shifting the minimum point to the left, hence the negatively biased time constant estimates. While, the NMSE CR algorithm is essentially unbiased for broadband temperature fluctuations, in practise the user will not have control over the frequency spectrum of the signals being measured. Consequently, in general, NMSE CR will produce negatively biased estimates.

Reducing estimation bias in CR blind characterisation algorithms, or eliminating it completely, through appropriate formulation of the cross-relation cost function, is the subject of ongoing research.

## REFERENCES

Cambray, P. (1986). Measuring thermocouple time constants: A new method. *Combustion Science Technology*, **45**, pp. 221–224.

Hung, P., S. McLoone, G. Irwin and R. Kee (2005). A difference equation approach to two-thermocouple sensor characterisation in constant velocity flow environments. *Review of Scientific Instruments*, **76**, Paper No. 024902.

Hung, P., S. McLoone, G. Irwin and R. Kee (2007). Blind deconvolution for two-thermocouple sensor characterisation, *Transactions of ASME*, **129**, pp. 194-202.

Kee, R. J., P. G. O'Reilly, R. Fleck and P. T. McEntee (1999). Measurement of exhaust gas temperature in a high performance two-stroke engine. *Transactions of SAE Journal of Engines*, **107**, SAE Paper No. 983072.

Liu, H., G. Xu and L. Tong (1993). A deterministic approach to blind identification of multichannel FIR systems. *Proceedings of 27th Asilomar Conference on Signals, Systems and Computers*, Asilomar, CA, pp. 581-584.

Pfriem, H. (1936). Zue messung verandelisher temperaturen von ogasen und flussigkeiten. *Geb. Ingen.*, **7**, pp. 85-92.

Strahle W. C. and M. Muthukrishman (1976). Thermocouple time constant measurement by cross power spectrum. Journal of AIAA Technical Notes, **14**, pp. 1642–1644.

Tagawa, M., T. Shimoji and Y. Ohta (1998). A two-thermocouple probe technique for estimating thermocouple time constants in flows with combustion: in situ parameter identification of a first-order lag system. *Review of Scientific Instruments*, **69**, pp. 3370-3378.

Tagawa, M., K. Kato and Y. Ohta (2003). Response compensation of temperature sensors: frequency-domain estimation of thermal time constants. *Review of Scientific Instruments*, **74**, pp. 3171-3174.

Tsuji, T., Y. Nagano, and M. Tagawa (1992). Frequency response and instantaneous temperature profile of cold-wire sensors for fluid temperature fluctuation measurements. *Experiments in Fluids*, **13**, pp. 171-178.

Xu, G., H. Liu, L. Tong and T. Kailath (1995) A least-squares approach to blind channel identification. *IEEE Transactions on Signal Processing*, **43**, pp. 2982-2993.